

Visualization of the flow field of a micro air vehicle in imitation of 8 stroke flapping movements

Conference Paper**Author(s):**

Zhang, Yiyuan; Kitagawa, Kazutaka; Konishi, Yasuhumi

Publication date:

2018-10-05

Permanent link:

<https://doi.org/10.3929/ethz-b-000279221>

Rights / license:

In Copyright - Non-Commercial Use Permitted



▪ Visualization of the flow field of a Micro air vehicle in imitation of 8 stroke flapping movements

Yiyuan Zhang^{1,c}, Kazutaka Kitagawa², Yasuhumi Konishi³

¹ Graduate student, Aichi Institute of Technology, Toyota, Aichi 470-0392, Japan

² Dept. of Mechanical Engineering, Aichi Institute of Technology

³ Institute of Fluid Science, Tohoku University, 9808577 Sendai, Japan

^cCorresponding author: Tel.: +81565488121; Fax: +81565484555; Email: p17713pp@aitech.ac.jp

KEYWORDS:

Main subjects: Flow visualization

Fluid: Bio fluid, Low speed flow

Visualization method(s): Smoke wire

Other keywords: Aerodynamic force measurement, Micro aerial vehicle, Biomimetic

ABSTRACT: *Micro aerial vehicle (MAV) is projecting to develop on unmanned missions to inspect the damage situation from a disaster such as an earthquake, a fire and radioactive pollution. MAV will be able to fly at low speed for the similarity of the birds and the insect's flight condition. This research is aiming for the design and development of a flapping mechanism with 8 stroke movements for hovering function in a narrow space. The present study is investigating to the characteristic of 8 stroke flapping movements from the measurement of aerodynamic force and smoke wire flow visualization.*

1 Introduction

Recently, the research and development of Micro air vehicles (also known as MAV) from the improvement of technology in biomimetic attracted the attention of various countries. With the expectation, to confirm a situation of damage and search for inside building collapse and an automobile crash and train accident from the natural disasters or human disasters. MAV's has a lightweight and a wingspan less than about 200 [mm] in imitation of insects and small birds in the natural world, such as the dragonfly, butterfly, beetle and hummingbird. MAV has to flight speed slower than 3 m/s corresponding to the Reynolds number of $Re \approx O(10^3) \sim O(10^4)[1] \sim [3]$. The live animal flights were good at hovering flight, a steep turn and steep dive. To manufacture the MAV, the biomimetics are used as some effective methods. Through the analysis of the flapping movement from live insects, the MAV flapping system has been designed in 8 stroke flapping movements which are often seen in common to hummingbird during hovering flight. Since flying in nature are producing their own vortex to help flying, it is important to visualize the air flow around the MAV. Present report is introducing to the characteristic of 8 stroke flapping movements by the measurement of aerodynamic force and smoke wire flow visualization.

2 Outline of the MAV flapping mechanism

Figures 1(A), 1(B) and 1(C) show the present flapping device. The flapping device consisted a couple of wings, a micro motor, small universal joints, spur gears and frame, as shown in Figs. 1(A) and 1(C). In Fig. 1(B), the geometry of wing profile used 90 mm in span length, 33.14 mm in the mean aerodynamic chord, 2181 mm² in wing area and aspect ratio $AR=6.0$, respectively. The total mass of

MAV has 10.24 g. The stroke-angle (between T.D.C-B.D.C) the 120 deg and the flapping frequency $f = 6.7$ Hz when motor applied a input voltage in 8 V under uniform flow velocity at 1.45 m/s.

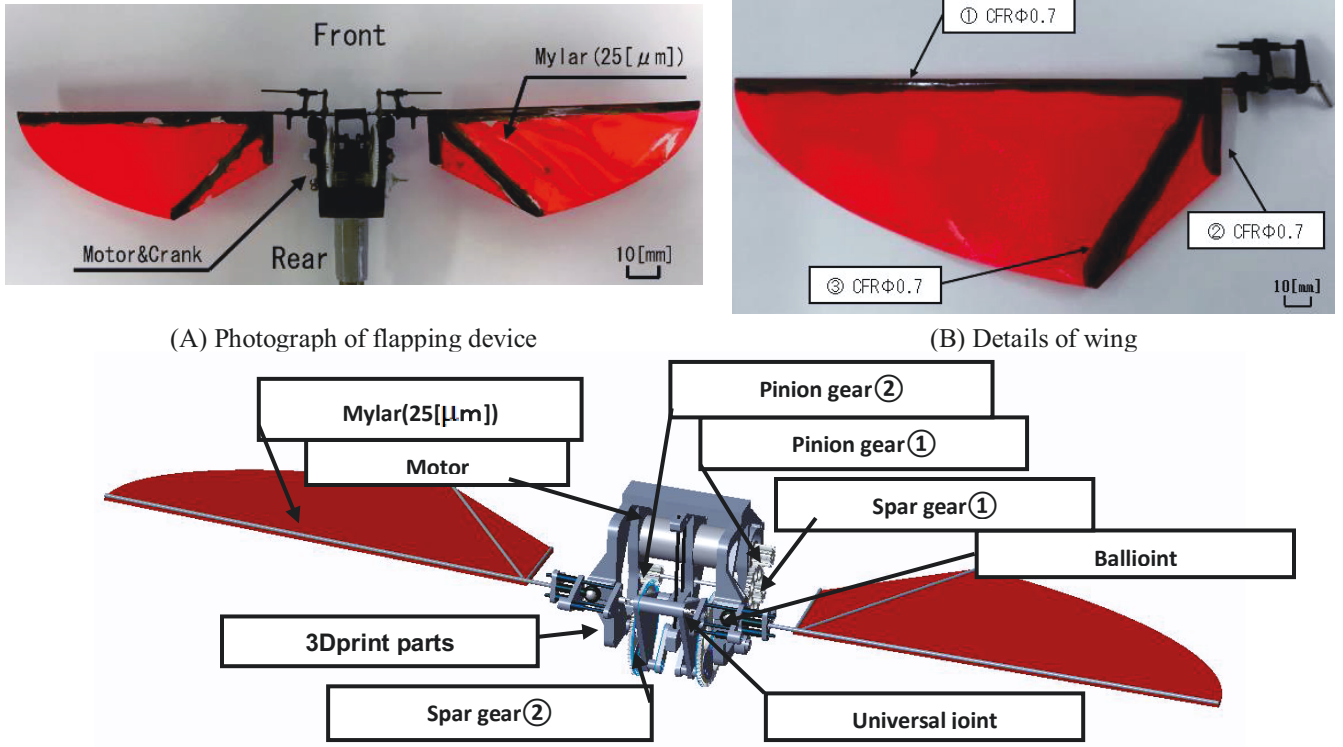


Fig. 1. Schematic description of flapping device

The chord Reynolds number Re and the reduced frequency k is defined as the following expressions[4]

$$Re = \frac{c_m U_e}{\nu} \quad (1)$$

$$k = \frac{2\pi f c_m}{U_{ref}} \quad (2)$$

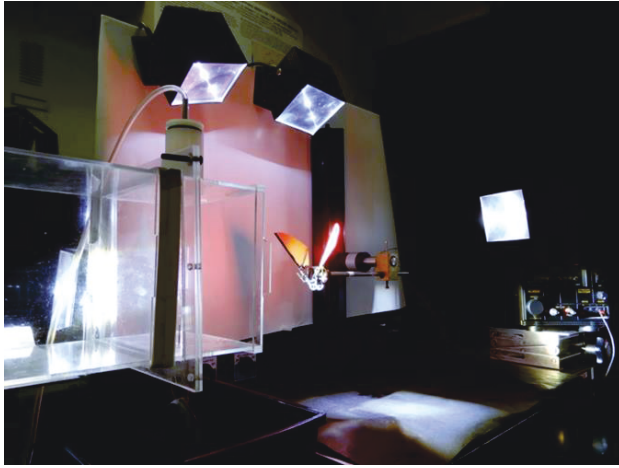
c_m denotes the mean aerodynamic chord ($=33.14$ mm), U_e the relative flow velocity in mean aerodynamic chord ($=0.3 \sim 0.6$ m/s), ν the kinematic viscosity, f the flapping frequency, and U_{ref} the average relative flow velocity at the wing tip ($=8.6$ m/s). As results of Re and k have $1.8 \sim 3.5 \times 10^3$ and 0.44, respectively. Results show that the flight phenomenon of MAV has in the range of the closely phenomenon of insect in the natural world.

3 Visualization of 8 stroke flapping movement on the wing flip

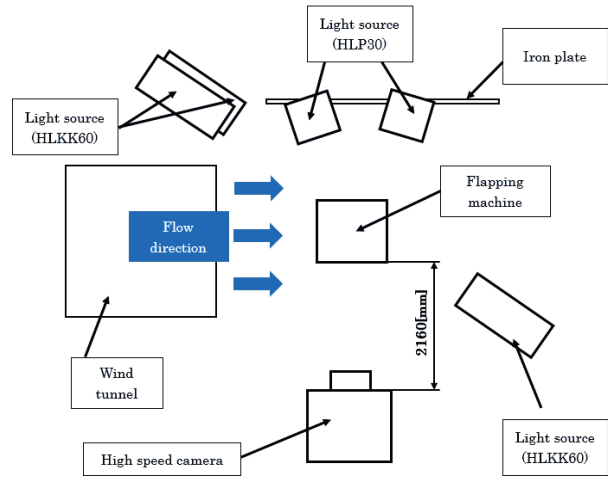
Figures 2(A) and 2(B) show the outline of visualization of flapping motion. In Fig. 2(A), the MAV is tethered a column of steel having a diameter of 8 mm and 230 mm in length. The flapping movement of MAV has been taken in windless condition by the high-speed camera with 105 mm macro lens at a distance of 2160 mm, as shown in Fig. 2(B). The shooting was performed at a frame rate of 2,000 fps, a shutter speed of 1/2,000 s, and a shooting resolution of 768×528 pixel (view field of 256.25×175

Visualization of the flow field of a Micro air vehicles in imitation of 8 stroke flapping movements

mm). The position of the camera needs adjustment according to the experimental environment. The light sources installed by two 30 W and three 60 W of LED lamps (Pi-PHOTONICS).



(A) Photograph of experimental condition



(B) Block diagram of experimental setup

Fig. 2. Outline of visualization of flapping motion

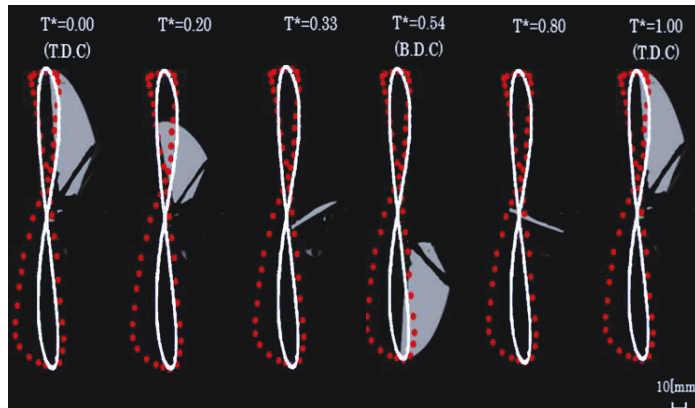


Fig. 3. Sequential photographs of a cycle of 8 stroke flapping movement

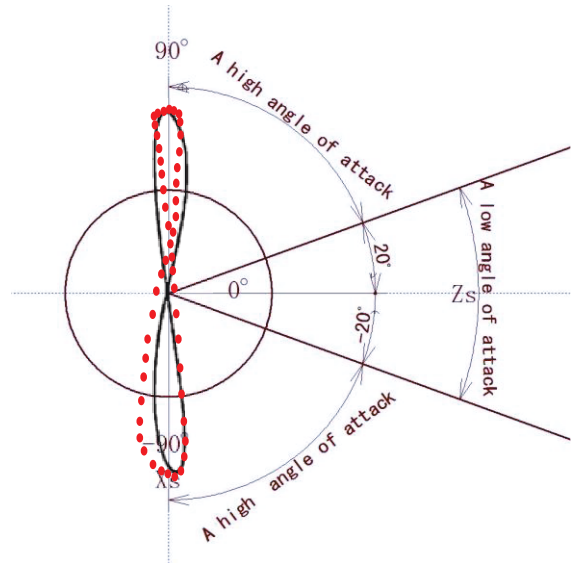


Fig. 4. Definition of angle of attack

The path of the wing tip traced by the points, and the solid line 3D simulation result, as shown in Fig. 3. Dimensionless elapsed time T^* is defined as a divided by one period of the flapping movement. The angle of attack under 20 deg in the counter clock wise(C.C.W) with respect to the Z_s axis is defined as a low angle of attack, and the angle over 20 deg in the clock wise(C.W) is defined as a high angle of attack, as shown in Fig. 4.

In Fig. 3, the MAV is successfully achieved the 8 stroke flapping movement when motor applied a input voltage of 6 V, which the flapping frequency is of 6.2 Hz. Downstroke is starting at $T^*=0$ from T.D.C. Comparison between the experimental and the simulation result is different in movement of passes ahead by the influence of fluid force during $T^*=0.15$ to $T^*=0.20$. Simulation is better be a high angle of attack at $T^*=0.33$, however, the wing has affected by the aerodynamic forces with low angle of attack. Upstroke is starting at $T^*=0.54$ from B.D.C. During the upstroke process, the trajectory during $T^*=0.54$ to $T^*=0.80$ is greatly shifted from the solid line, because of the feathering movement by the elastic deformation of the wing did not occur near the T.D.C and B.D.C. A flapping cycle complete with $T^*=1.0$, and the ratio of the upstroke to the down stroke (stroke ratio) was 0.85. The aerodynamic force during downstroke process could occur more than the force during the upstroke process, which made the downstroke process took longer than the upstroke process.

4 Aerodynamic forces experiment

Since the flight state of MAV is close to the hovering flight of the hummingbird, by using the air flow to generate the lift force. The aerodynamic force was measured in the horizontal direction. Figure 5 shows the schematic description of the aerodynamic force measurement. Flapping machine is tethered a column L-shaped cantilever in 8 mm Dia. with the length of 140 mm and 530 mm, respectively. The strain gauges were used KFG universal foil strain gauge KFG-5-120-C1-11 (resistance value: 120 Ω , gage ratio: 2.1). The bending surface strain on a round bar was measured by the 2 gauge method. The strain gauge has been attached at a position by 255mm away from the center axis of the MAV. $100 \times 100 \times 10^{-6} \epsilon$ in the sensitivity of the dynamic strain gauge, and 30 Hz in low pass filter. The camera was synchronized with an oscilloscope to control the trigger with an external electric signal. The experiment was carried out under a windless condition with motor applied the input voltage of 4, 8 and 10 V.

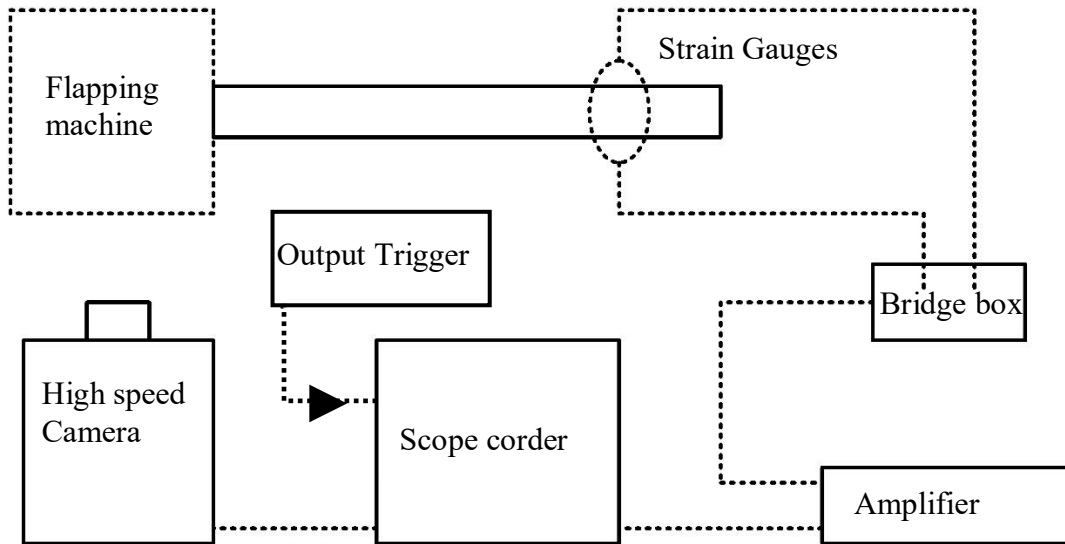
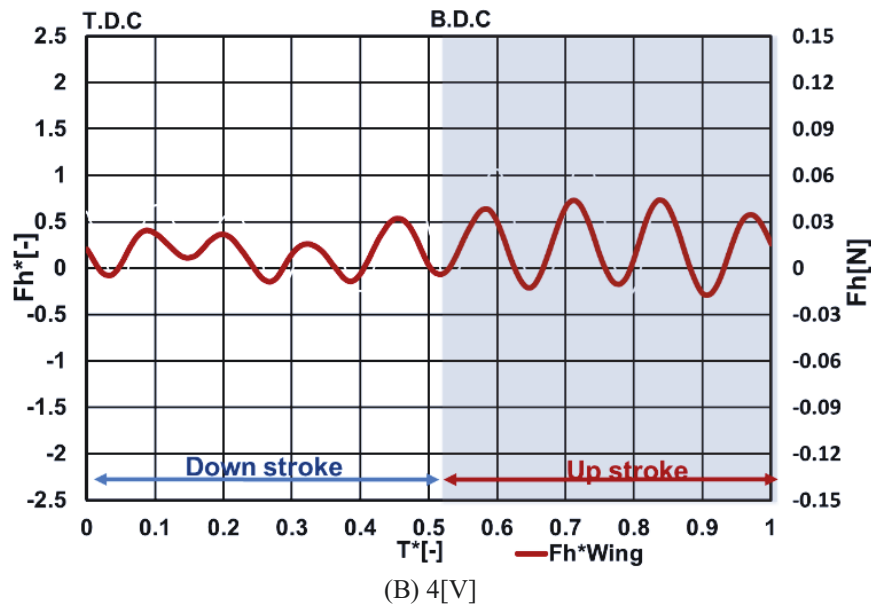
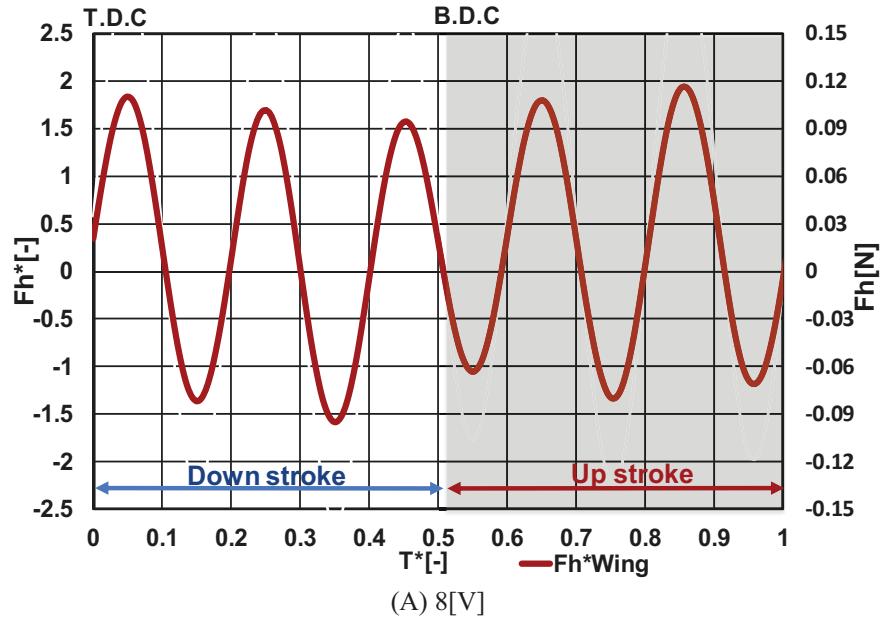


Fig. 5. Details of aerodynamic force measurement system

Figure 6(A), 6(B) and 6(C) show the time history of the aerodynamic force Fh^* . The dimensionless horizontal force Fh^* is defined as the aerodynamic forces divided by the weight of the MAV. In Fig. 6(A), the average Fh^* and flapping frequency under one period of the flapping movement are evaluated

Visualization of the flow field of a Micro air vehicles in imitation of 8 stroke flapping movements

as 0.236 and 6.7 Hz for the input voltage of 8 V. The maximum value of F_h^* during the downstroke is 1.84 at $T^*=0.04$. While the maximum value of F_h^* during the upstroke is 2 at $T^*=0.85$. The aerodynamic force is stabilized from each stroke. However, the feathering movement by the elastic deformation of the wing near the top dead center and bottom dead center was not executed, the vortex produced by the wing could be wasted. In Fig. 6(B), the average force F_h^* and flapping frequency under 4 V were evaluated about 0.202 and 4.07 Hz, respectively. In Fig. 6(C) these values at 10 V have 0.228 and about 7.06 Hz. At the 10 V, The wing could not against more aerodynamic force produced from the wing because of the destruction of the wing. All results of flapping frequency were less than 18 Hz from design calculation. Forcing on the changes in voltage and flapping frequency, the low flapping frequency could generate low aerodynamic force, and required to increase more vibrations in one cycle. Thus aerodynamic force could be affected on the flapping frequency greatly.



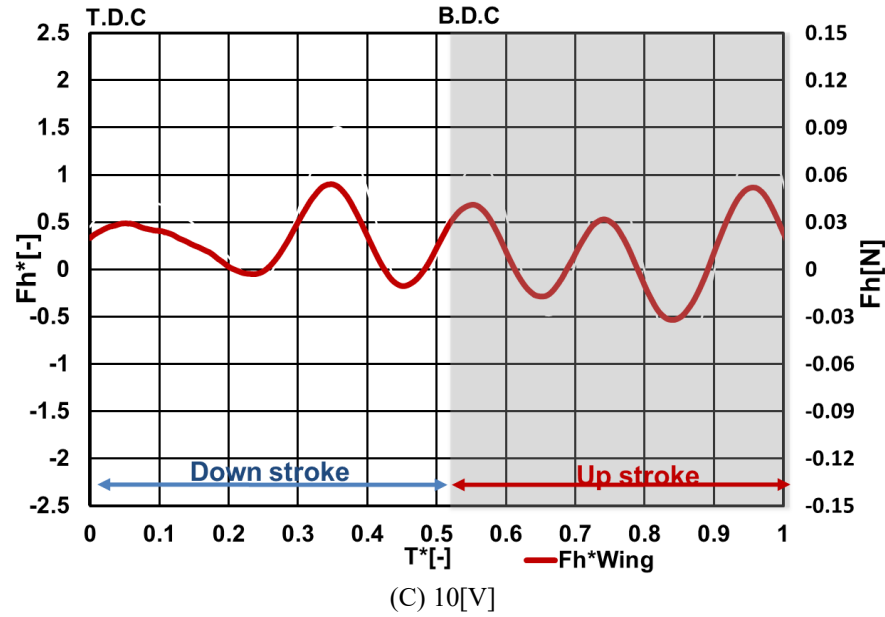


Fig. 6. Time history of aerodynamic force

5 Visualization of the flow field of MAV

The visualization of the flow field of a MAV in imitation of 8 stroke flapping movements performed by a smoke wire method. Figure 7 shows the schematic description of low speed wind tunnel. Flow channel is made by acrylic plates to visualize the flow around the MAV. The inside shape of the wind tunnel has a square cross section of 150×150 mm, and 1,610 mm in total length. The rectifier pipe used the aluminum honeycomb (cell size 3.18 mm) manufactured by Showa Aviation Industry Co.Ltd. The test specimen is tethering at 100 mm from the wind tunnel exit. Figure 8 shows the photograph of 2 smoke wire method, the system composed of a droplet mechanism, a transformer, a bridge circuit, a nichrome wire, and an air valve. The smoke wire is knitted in three-ply nichrome wires with a diameter of 0.1 mm. The oil is used for liquid paraffin and a kinematic viscosity of $200 \sim 250$ m²/s. The oil was coated thinly and a tiny drop on the nichrome wires and electrically heated to generate smoke wire streaks.

Visualization of the flow field of a Micro air vehicles in imitation of 8 stroke flapping movements

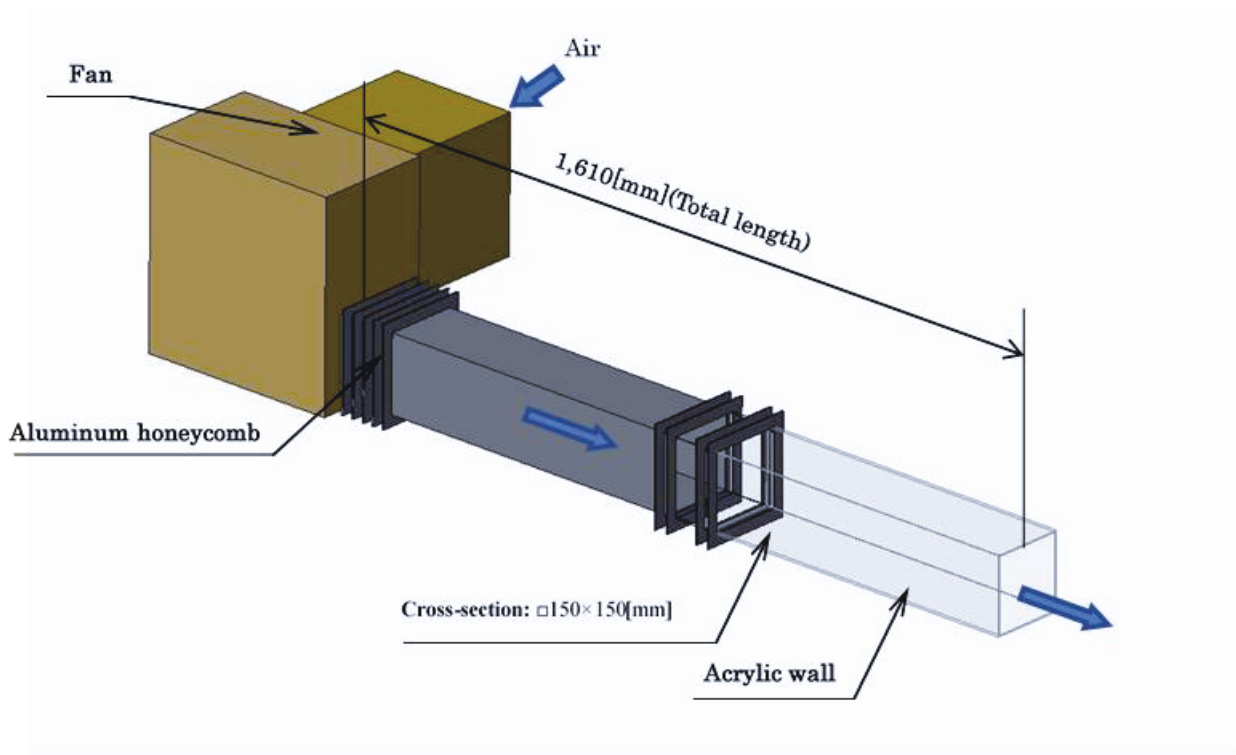


Fig. 7. Photograph of low speed wind tunnel

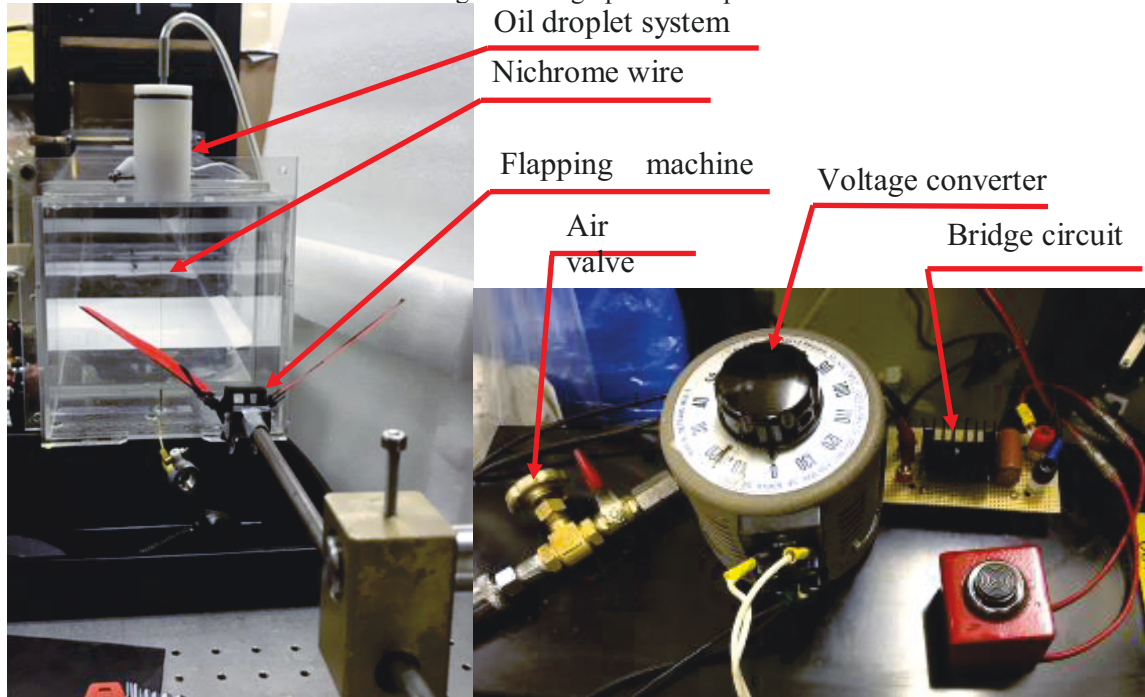


Fig. 8. Schematic description of 2 smoke wire method

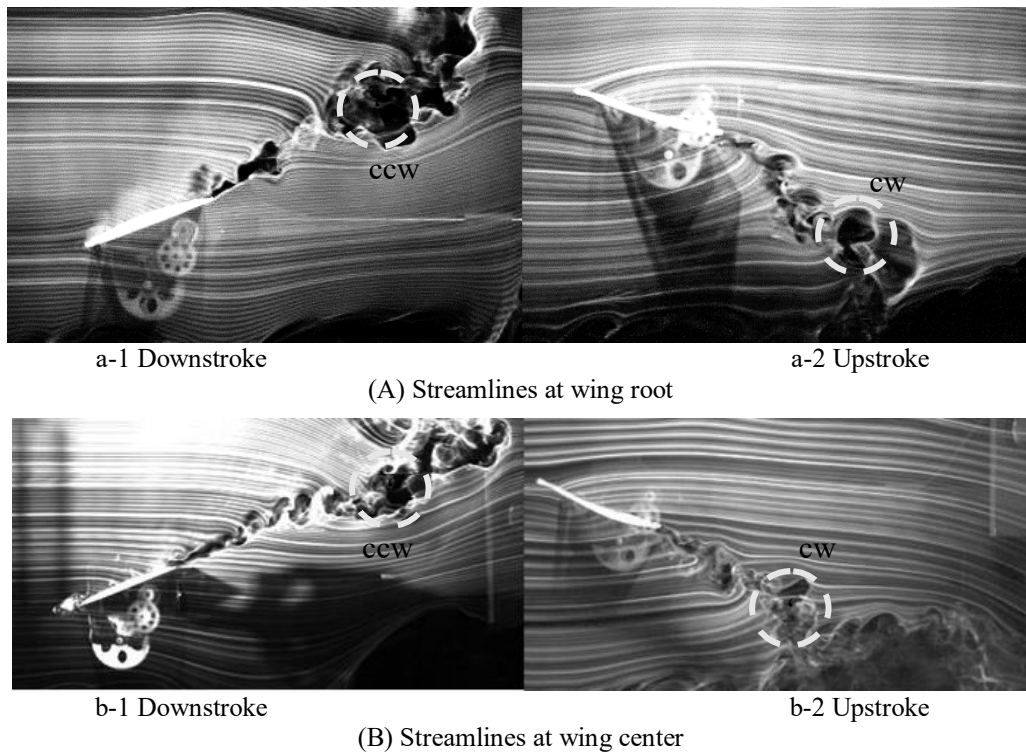


Fig. 9. Visualization around view area from side of MAV

Figures 9(A) and (B) show typical smoke-streak flow patterns on around the fixed wing for several angles of attack (AOA). In Fig. 9(A) a-1, during the downstroke process, the streamlines at wing root were cutting through by the leading edge of the wing, the cutted streamlines went around to the wing upper surface and moved out from the trailing edge. The streamlines from the trailing edge were giving turbulence in the flow and formation of vortexes. The vortex structure has grown in C.C.W, separated in accordance with downstream. In Fig. 9(A) a-2, during the upstroke process, the streamlines at wing root were cutting through by the leading edge of the wing, the cutted streamlines went around to the wing upper surface and moved out from the trailing edge without separation. The streamlines from the trailing edge were giving turbulence in the formation of vortexes. The vortex structure has grown in C.W, left and collapsed in accordance with downstream. The streamlines in Fig. 9(B) show results of the downstroke process and the upstroke process at wing center. At the downstroke and upstroke process, the smoke-streak flow patterns visualized and growth of vortexes similar to Fig. 9(A) a-1 and 9(A) a-2. Figure 10 shows the sequential streamlines image of a cycle of flapping motion, peeling eddies could be confirmed at trailing edge of the wing during downstroke and upstroke, however, the feathering movement by the elastic deformation of the wing near T.D.C and B.D.C did not occur, the utilization of the vortexes produced by wings was failed.

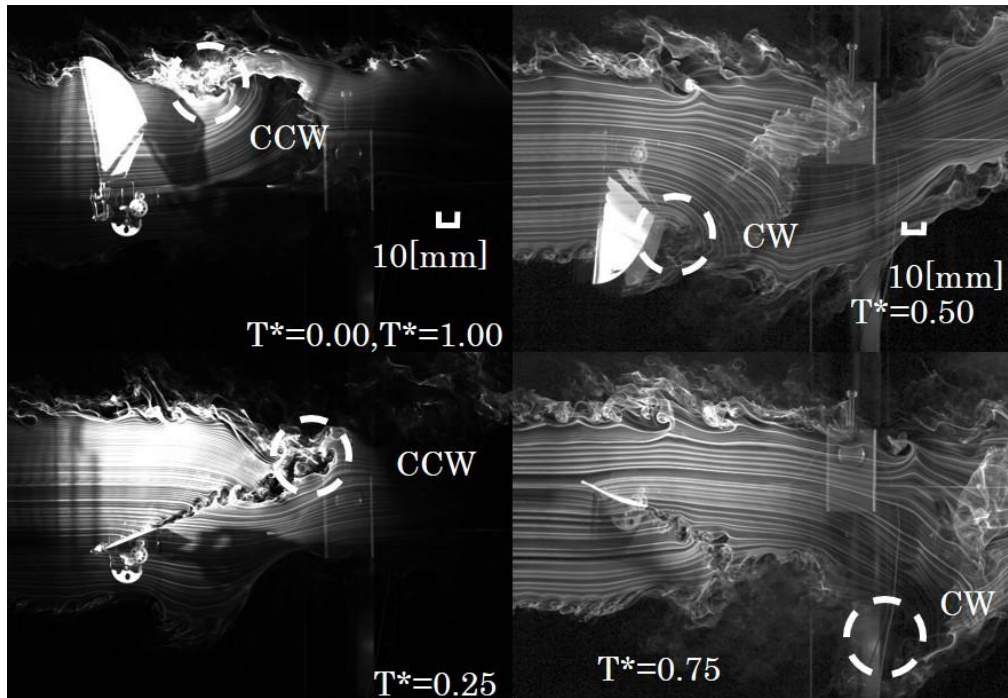


Figure. 10. Smoke wire visualization of the air flow around the flapping wing

6 Conclusion

Visualization of air flow around flapping wing and measurement of aerodynamic force in 8 stroke flapping movements by experiment investigation, the results of present study summarized as follows:

- (1) The flapping movement has been confirmed in 8 stroke flapping movements, which is extremely close to the design simulation trajectory. During upstroke process, the trajectory greatly shifted from the simulation, because of the feathering movement by the elastic deformation of the wing could not confirm near the T.D.C and B.D.C.
- (2) From aerodynamic force measurements, the average of one cycle $Fh^* = 0.236$, under the input power of 8V, which was possibility shown the production of lift force. The aerodynamic force could be greatly affected by the flapping frequency, the improvement of flapping frequency is necessary to obtain greater aerodynamic force.
- (3) The smoke-streak flow patterns were visualized attached surface flow, production of the vortexes and separation near trailing edge. During the flapping movement, the feathering movement could help to occur more aerodynamic force by using the formation of vortexes. However, the vortexes were collapsed in accordance with downstream from the trailing edge. The development of wing with feathering motion by the elastic deformation which can withstand the stronger aerodynamic force is necessary.

References

- [1] Azuma A. biological movement of the Encyclopedia, Asakura Shoten, (2007)
- [2] Azuma A. THE BIOKINETICS OF FLYING AND SWIMMING SECOND EDITION, *AIAA Education Series*, 2006.
- [3] WEI SHYY, et al, “An Introduction to FLAPPING WING AERODYNAMICS”, CAMBRIDGE, (2013)
- [4] Tatsuya Nomura, “Research and development of flapping mechanism to provide the motion of figure-eight pattern”, the 34th society of Aero Aqua Bio-mechanisms, pp.11~12, (2016)